Title

Searching for the QCD axion with the proposed International Linear Collider beam facility

Journal

Physical Review D, 106(5)

ISSN

2470-0010

Authors

Fukuda, Hajime

Otono, Hidetoshi

Shirai, Satoshi

Publication Date

2022-09-01

DOI

10.1103/physrevd.106.055029

Searching for the QCD axion with the proposed International Linear Collider beam facility

Hajime Fukuda,[1,2] Hidetoshi Otono,[3] and Satoshi Shirai[4]

[1]*Theoretical Physics Group, Lawrence Berkeley National Laboratory, California 94720, USA*
[2]*Berkeley Center for Theoretical Physics, Department of Physics, University of California, Berkeley, California 94720, USA*
[3]*Research Center for Advanced Particle Physics, Kyushu University, Fukuoka 819-0395, Japan*
[4]*Kavli IPMU (WPI), UTIAS, The University of Tokyo, Kashiwa, Chiba 277-8583, Japan*

(Received 1 April 2022; accepted 1 September 2022; published 21 September 2022)

One of the most promising methods to search for axions is a light-shining-through-walls (LSW) experiment. In this work, we discuss the possibility of performing a LSW experiment at the International Linear Collider facility, where photon beams are generated for positron production. The photon beam is energetic and intense; the energy is of order MeV and the number of photons is about 10^{24} per year. Because of the high energy and intensity, this LSW experiment can probe a parameter region of the axion unexplored by previous ground-based experiments.

DOI: 10.1103/PhysRevD.106.055029

I. INTRODUCTION

The International Linear Collider (ILC) [1] is a future electron-positron linear collider. Unlike a circular collider, storage and recycling of beam particles are not possible in a linear collider. To obtain a large luminosity, we need a positron source of strong intensity at the ILC. It is, however, challenging to develop a high-intensity positron source. One promising proposal is to use the main electron beam. In this proposal, the electron beam passes through a helical undulator before the interaction point. By the undulator, spatially oscillating magnetic fields are imposed and an intense photon beam is emitted from the electron beam. The photon beam then goes through a thin target, generating e^+e^- pairs [2]. In order to generate abundant positrons at the ILC, the photon beam from the undulator must be sufficiently intense and energetic. Indeed, it is the strongest MeV photon beam available on the ground up to the present. However, after the electron-positron pair creation, the photon beam is not used anymore but dumped in the current design.

In this work, we propose to use this photon beam for a search for new light particles, in particular, axions. An axion is a pseudo Nambu-Goldstone boson associated with the spontaneous breaking of a global $U(1)_{PQ}$ symmetry, which is anomalous on the QCD sector. It is introduced to solve the strong CP problem in the standard model (SM) [3–6], where the θ angle in the QCD Lagrangian is unnaturally small [7]. It is one of the most important targets for physics beyond the SM. Because of various experimental constraints, the scale of the $U(1)_{PQ}$ symmetry breaking should be much larger than the electroweak scale. Prime examples of such invisible axion models are the Kim-Shifman-Vainshtein-Zakharov (KSVZ) [8,9] and Dine-Fischler-Srednicki-Zhitnitsky (DFSZ) [10,11] models. With the color anomaly of the $U(1)_{PQ}$ symmetry, an axion couples to gluons. After the QCD phase transition, the axion-gluon coupling induces mixings between the axion and mesons, resulting in the axion mass. The axion also couples to photons from the dynamics of the $U(1)_{PQ}$ symmetry breaking sector and the mixing with mesons.

In the presence of a magnetic field, the axion-photon coupling induces mixing between an axion and a photon; a photon can oscillate into an axion and vice versa [12]. A type of experiment to use this oscillation to detect an axion is called a light-shining-through-walls (LSW) experiment [13,14]. In LSW experiments, a photon detector is placed far away from a photon beam source in the beam direction. Between the detector and the beam source, a thick wall is placed to shield the photon beam. Magnetic fields perpendicular to the beam direction are imposed along the way between the photon beam source and the detector. If the mixing between the axion and photon is large enough, the photon from the source can convert into an axion before the wall, and the axion penetrates the wall. The axion after the wall may oscillate back to a photon by the magnetic field again. The reconverted photon is observed by the detector. In this way, LSW experiments can detect axion particles. LSW experiments are one of the

most promising ways to search for axions and a number of experiments have been performed [15–23].

Our proposal is to perform a LSW experiment at the ILC by using the MeV photon beam for positron production. The photon dump in the ILC plays the role of the thick wall in a LSW experiment. The dump can be placed about 2 km away from the undulator [24]. We propose to install magnets in the vacancy before and after the dump to induce the photon-axion mixing. The converted "axion beam" is invisible and goes through the dump. The axions oscillate back to photons, being observed at the photon detector. As the photon beam is well collimated and the opening angle is of order of the inverse of the Lorentz factor of the main electron beam, $O(10^{-6})$ rad, the beam spread is less than centimeters even at distances of more than 1 km. This makes it possible to efficiently impose a magnetic field to the axion/photon beam over several kilometers or even more. Depending on the details of the experiment, such as the tunnel structure, it is possible to apply a magnetic field inside the ILC tunnel and its extension, or it is also possible to apply a magnetic field on the ground to the beam coming through the ground. We can thus construct a LSW experiment using the ILC facilities.

This paper is organized as follows: in Sec. II, we discuss the conversion probability between an axion and a photon and show the advantage to use the MeV photon beam at the ILC for the LSW experiment. We discuss experimental setups in Sec. III and show the expected sensitivities in Sec. IV. Finally, Sec. V is devoted to the conclusion and discussion.

II. OPTIMIZATION OF AXION-PHOTON CONVERSION

With the existence of a time-independent magnetic field B in z direction, the conversion probability between an axion with an energy ω and a mass m_a to a photon with a given polarization vector e is

$$P(a \to \gamma; \omega) \simeq \frac{g_{a\gamma\gamma}^2}{4} \left| \int dz e^{iqz} \vec{B}(z) \cdot \vec{e}(k) \right|^2, \qquad (1)$$

as we derive in the Appendix. Here, $g_{a\gamma\gamma}$ is the coupling constant between an axion and two photons, defined in Eq. (A2), and $q = \omega - \sqrt{\omega^2 - m_a^2}$ is the momentum transfer between the photon and axion.

For a spatially constant magnetic field, $B_x(z) = B_0$, the formula reduces to

$$P(a \to \gamma; \omega) = \frac{1}{4} g_{a\gamma\gamma}^2 B_0^2 L^2 \left[\frac{\sin(qL/2)}{qL/2} \right]^2, \qquad (2)$$

where L is the distance over which the magnetic field is imposed for the axion-photon conversion. For $\omega \gg m_a$, the momentum transfer q is

$$q \simeq \frac{m_a^2}{2\omega} = (10\ \text{km})^{-1} \left(\frac{m_a}{10^{-2}\ \text{eV}} \right)^2 \left(\frac{2.5\ \text{MeV}}{\omega} \right). \qquad (3)$$

For a smaller value of the momentum transfer $q \ll 1/L$, larger values of L can enhance the conversion rate. However, for $qL \gtrsim 1$, the conversion rate gets smaller and is suppressed by q^{-2}. In terms of the axion mass, the conversion rate becomes smaller for $m_a \gg \sqrt{\omega/L} \sim 10^{-4}\ \text{eV}(\omega/1\ \text{eV})^{1/2}(L/1\ \text{m})^{-1/2}$. Therefore, LSW experiments using visible laser beams, $\omega = O(1)$ eV, do not have a good sensitivity to the high-mass part of the QCD axion parameter space.

There are several ways to improve the sensitivity for the heavier mass region, $m_a = O(0.1\text{–}1)$ eV. First, one can use photons with higher energy. This suppresses the momentum transfer and we may have longer $L \lesssim 1/q$. As we will see later, the energy of the undulator photons at the ILC can be $O(10)$ MeV, allowing one to maintain the sensitivity to sub-eV QCD axions even for $L \sim$ km.

Second, we may adopt magnetic fields wiggled spatially with a period of $O(1/q)$ to further improve the heavier-mass sensitivity. In this case, the integral of the conversion rate (A7) is no longer canceled for $qL \sim 1$ and the conversion rate can be enhanced for larger distance L. For example, if $B(z) = B_0 \sin(zq)$, the conversion probability $P \propto (B_0 L)^2$ and is not suppressed for higher axion masses. Finally, we may also give an effective mass ω_p to the photon to suppress the momentum transfer [25–27]. This can be done by filling the whole conversion volume with, for example, helium gas. However, it is not obvious whether a small plasma frequency of order $\omega_p \sim m_a = O(0.1\text{–}1)$ eV affects the coherent oscillation between a photon and an axion as energetic as $O(10)$ MeV. Moreover, the gas would absorb photons and a longer conversion length could not be used. Thus, we do not adopt this method in this work.

Another important target at LSW experiments is a dark photon γ', a hypothetical massive vector boson with non-vanishing kinetic mixing χ with a SM photon. With this mixing χ, the interaction and energy eigenstates of the vector bosons are not identical. As a result, a photon, the SM interaction eigenstate, oscillates into a dark photon, the hidden interaction eigenstate with a momentum p, and vice versa, even without any external fields like magnetic fields. In the dark photon search, the use of a high-energy photon beam is expected to enhance the sensitivity for heavier dark photon mass regions [28]. However, the precise upper bound on the dark photon mass is not clear for the following two reasons. First, the mass threshold, in other words, $\sqrt{s}$, of the photon creation process is not clear. It depends on the detailed design of the undulator. Second, for larger dark photon masses, the different mass eigenstates decohere; a vector boson at the source is not the SM interaction eigenstate but a mixed state of the mass

eigenstates. To estimate the decoherence effect, we need to take into account how localized wave packets are [29]. We leave the analysis of the dark photon for future work.

III. EXPERIMENTAL SETUP

A schematic picture of our proposal is shown in Figs. 1 and 2, assuming the undulator-based positron source [30]. Detailed information on the ILC site is found in, for example, Ref. [31]. The main electron beam passes through a helical undulator to produce gamma rays with energies around 10 MeV. Subsequently, the photons impinge on a thin target to produce positrons. We propose to use the photon beam after the target as the source of a LSW experiment for the axion search. In the present design of the ILC, the photon beam pipe will be installed about laterally 1.5 m away from the electron main beam pipe. We thus may install magnets and apply a magnetic field on the photon beam in the section between the photon dump and the target. The magnetic field induces the photon-axion mixing and a fraction of photons are converted into axions, passing through the photon dump. We impose a magnetic field behind the dump to turn the axions back into photons again, which are then captured by the detector.

The advantage of performing a LSW experiment using the ILC photon beam is the high photon energy; as discussed in Sec. II, the sensitivity to heavier axions does not decrease even if a magnetic field is applied over a long distance. To improve the sensitivity to heavier axions further, we also propose to make the magnetic field spatially periodic.

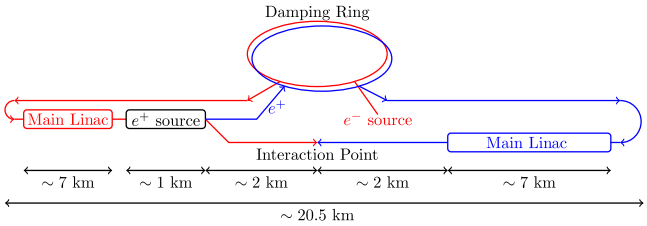

FIG. 1. Rough dimensions of the whole ILC system based on Ref. [32].

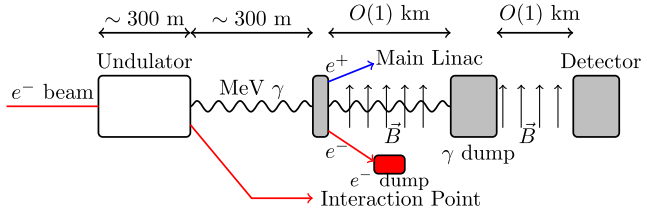

FIG. 2. A schematic of the positron production system at the ILC based on undulator photons and proposed LSW experiment for the axion detection.

A. The undulator photon beam

Let us review the photon beam system at the ILC [30]. For the ILC250 main electron beam, the pulse repetition rate is 5 Hz and each pulse contains 1312 bunches containing $\sim 2 \times 10^{10}$ electrons with a bunch separation of 554 ns and a bunch length 0.3 mm. In the design proposal, the undulator period is $\lambda = 11.5$ mm and the undulator parameter is $K \equiv eB\lambda/2\pi m_e = O(1)$. The typical energy of the undulator photons is $\omega \sim 4\pi\gamma_e^2/(1 + K^2)\lambda$ with γ_e being the Lorentz factor of the electrons. The opening angle of the beam is around $1/\gamma_e = O(10^{-6})$. The photon beam power is $O(10 - 100)$ kW. The photon beam is well collimated, so even if it flies several kilometers, its spread is $O(1)$ cm. As the electron beam has a pulsed structure, the photon beam has the structure as well, which is important to reduce the background as will be discussed below.

The undulator photons impinge on a thin target to generate positrons. A few percent of the photons from the undulator are absorbed in the thin target and the rest passes through. The remaining photons are absorbed in a photon dump system. The photon dump is proposed to be placed about 2 km away from the undulator, as the divergence of the photon beam can mitigate the temperature rises of the beam window [24]. For the ILC250, we propose to use the space between the source and the dump as the "conversion distance," where a photon converts into an axion in a magnetic field; i.e., we propose to impose magnetic fields over 2 km.

B. Photon detector

The location of the reconversion path and the photon detector depends on the details of the ILC tunnel and beam design. The ILC tunnel will not be straight as it follows the curvature of Earth and there is a nonzero crossing angle at the collision point. There are several possible locations for the reconversion pipe. Here we discuss the possibility of installing the reconversion pipe and the detector in a different tunnel than the ILC main tunnel, which turns out to be an underground low-level counting experiment.

The signal of the experiment is a single photon with an energy of around 10 MeV, while cosmic rays could be the main sources of background: either via neutrons from the negative muon capture or from direct ionization in the detector. Radionuclides in the detector environment do not contribute to the background, since the energy of photons from the radionuclides would not be more than 3 MeV. Reference [33] shows that a simple 76-mm-diameter and 76-mm-long high-purity germanium (HPGe) radiation detector located in an underground laboratory at 20 m water equivalent recorded 1 count/day/MeV around 10 MeV if additional detectors for the anticosmic suppression are installed (see Fig. 2.15 in the Ref. [33]). Since the location of the photon detector for

the experiment is supposed to be at about 200 m below the surface of the ground, the muon flux could be attenuated by a factor of 10^{-3} (see Figs. 1.3 and 2.9 in the reference). As discussed before, the photon beam has a pulsed structure. The timing information can be used to suppress backgrounds even further. The intrinsic time resolution of HPGe detectors is expected to be 3–4 ns [34], which provides a reduction factor of 10^{-4}. Consequently, the background is estimated to be negligible even for ten years running of the ILC250.

Moreover, we can also utilize the angular information of the photon. The photon from the axion should be collimated within a $O(1)$ cm radius at the detector location. Various position and angular sensitive detectors for MeV gamma rays are developed for astrophysical and medical applications. For example, the AMEGO detector [35] and e-ASTROGAM [36,37] would provide a position resolution around 1 mm and an angular resolution of around 1° at 10 MeV. This information can further suppress the background. In the following discussion, we assume the background can be zero and the detection efficiency of the photon is 100%.

IV. EXPECTED SENSITIVITY

Let us estimate the number of observed photons. For a photon with an energy ω and polarized in the direction of a magnetic field, the conversion rate is given by, as we have derived in the Appendix,

$$P(\gamma \to a;\omega) \simeq \frac{g_{a\gamma\gamma}^2}{4}\left|\int dz e^{iqz} B_1(z)\right|^2, \tag{4}$$

where $B_1(z)$ is the configuration of the magnetic field in the photon conversion region. Similarly, the reconversion from an axion to a photon is given by

$$P(a \to \gamma;\omega) \simeq \frac{g_{a\gamma\gamma}^2}{4}\left|\int dz e^{-iqz} B_2(z)\right|^2, \tag{5}$$

with $B_2(x)$ being a magnetic field in the reconversion region.

The undulator photons used in this experiment are not monochromatic but have a finite energy spectrum $\mathcal{F}(\omega)$, where the number of photons with energy from ω to $\omega + d\omega$ is $\mathcal{F}(\omega)d\omega$. The final result of the expected number of the photons $\mathcal{N}$ is given by

$$\mathcal{N} = \frac{1}{2}\int d\omega \mathcal{F}(\omega) P(\gamma \to a;\omega) \times P(a \to \gamma;\omega). \tag{6}$$

Here, an extra $1/2$ factor appears, as the ILC undulator photon is circularly polarized. In the following analysis, we adopt the photon spectrum $\mathcal{F}(\omega)$ from Refs. [38,39] and take $\omega > 5$ MeV to suppress the background from the radionuclides. As for the configuration of the magnetic fields, we consider the uniform and wiggled cases. For the wiggled magnetic field, we use a square wave with the spatial period $2w_B$, $B(z) = B_0 \times \mathrm{sgn}(\sin(\pi z/w_B))$, for simplicity.

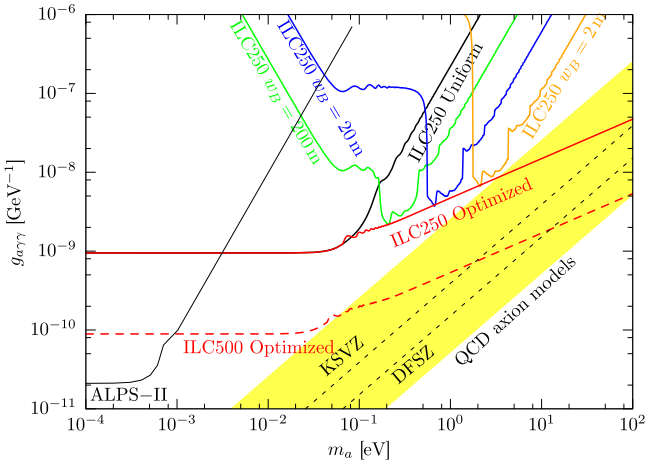

FIG. 3. The expected sensitivity of the ILC LSW experiment. The yellow region shows the range of the QCD axion models [40].

In Fig. 3, we show the expected detection sensitivity of the QCD axion at 95% C.L. assuming the background is zero, i.e., $\mathcal{N} = 3.0$. In the solid lines, we show the sensitivity of ten years running of the ILC250, which produces around 10^{25} undulator photons [38,39]. Here we assume that both lengths of the conversion distance and reconversion distance are 2 km and the amplitude of the magnetic field B_0 is 1 T. In addition to the uniform magnetic field, we show the magnetic field wiggled with $w_B = 200$, 20, and 2 m. In these cases, the sensitivity for the axion mass satisfying $qw_B = O(1)$ can be improved. Moreover, we also show the case that the value of w_B is optimized for each mass: $w_B = \pi/q \simeq 2\pi\bar{\omega}/m_a^2$, where $\bar{\omega}$ is a typical energy of the undulator photon and 7(16) MeV for the ILC250(ILC500). Note that for the axion mass $m_a \gtrsim 100$ eV, we need a small period $w_B \lesssim 1$ mm to keep the better sensitivity. In the dashed line, we represent the optimized case for the ILC500. Here we adopt 10 km conversion and reconversion distances and 2 T magnetic fields. The sensitivity for $g_{a\gamma\gamma}$ is approximately proportional to $1/(BL)$ and the longer conversion distance and stronger magnetic field can probe the larger axion decay constant. In this figure, we also show the sensitivity of the ALPS-II [16]. Compared with the LSW experiments based on optical or infrared lasers, the present LSW experiment at the ILC can probe higher mass axion.

V. CONCLUSION AND DISCUSSION

In this work, we have proposed a LSW experiment using a MeV undulator photon beam at the ILC beam facility. Our proposal requires one to install magnets along the photon beam line separated from a reconversion pipe and a photon detector by the photon dump, which acts as the wall.

Thanks to the high photon energies, we will be able to probe high-mass axions that have not been explored by ground-based experiments.

One of the advantages of the presented method is that it is highly expandable. Basically, the greater the length of the magnetic field applied, the better the sensitivity to the axion-photon coupling. If we adopt a magnetic field wiggled with a period $O(1)$ cm–$O(100)$ m, we can test even higher axion masses, which is a well-motivated parameter region as a solution to the strong CP problem. Also, our method may be applied for the other electron-positron colliders, such as the Compact Linear Collider [41], if an undulator-based positron source is used.

Of course, how long the magnetic field can be imposed and where the photon detector can be placed strongly depends on the detailed design of the ILC, such as tunnel and beam designs. Depending on these designs, they may be placed in the ILC tunnel itself or in its extension. For example, as we have discussed, the current design may admit to use a ∼2 km photon beam line as the conversion distance, but we need to modify the photon beam line design for the longer conversion distance. Another possibility for the reconversion pipe is to place it and the detector on the ground. After the photon dump, the invisible axion beam goes straight into the rock around the ILC tunnel. As is discussed in Ref. [31], the whole ILC tunnel is under mountains and the axion beam will eventually appear on the ground, although the precise location depends on the engineering details. As the photon/axion beam is well collimated, the size of the axion beam spread after can still be small on the ground. Thus an alternative way to set up a LSW experiment at the ILC is to install the reconversion magnets and the photon detector above ground, in the direction of the axion beam.

Finally, let us comment on the sensitivity at the ILC LSW experiment for the dark photon search γ'. With the nonzero kinetic mixing χ between the photon and dark photon, the conversion $\gamma \leftrightarrow \gamma'$ process can occur. As we have mentioned in Sec. II, in the case that the dark photon mass is comparable to the photon beam energy, it is difficult to estimate the conversion probability. For the dark photon of a mass much less than the photon energy, the conversion rate is $P(\gamma \leftrightarrow \gamma') \sim \chi^2$ and we estimate the ILC250 can reach $\chi \simeq 3 \times 10^{-7}$.

ACKNOWLEDGMENTS

We would like to thank Yu Morikawa for helpful discussions on the undulator positron source at the ILC. This work is supported in part by JSPS Grant-in-Aid for Scientific Research 17H02878 (S. S.), 18K13535 (S. S.), 19H04609 (S. S.), 20H01895 (S. S.), 20H05860 (S. S.), and 21H00067 (S. S.) and by World Premier International Research Center Initiative (WPI Initiative), MEXT, Japan (S. S.) by the Director, Office of Science, Office of High Energy Physics of the U.S. Department of Energy under the Award No. DE-AC02-05CH11231 (H. F.).

APPENDIX: AXION-PHOTON CONVERSION PROBABILITY

In this appendix, we discuss the axion-photon conversion probability. In the interaction picture, the axion-photon conversion probability in the presence of the magnetic field is

$$P(a \to \gamma) = \frac{|\langle a(p)|T\exp(-i\int H_I dt)|\gamma(k)\rangle|^2}{\langle a(p)|a(p)\rangle\langle\gamma(k)|\gamma(k)\rangle}, \quad \text{(A1)}$$

where $p(k)$ is the four momentum of the axion (photon) and H_I is the interaction Hamiltonian,

$$H_I = \int d^3x \frac{1}{4} g_{a\gamma\gamma} a F_{\mu\nu}\tilde{F}^{\mu\nu}. \quad \text{(A2)}$$

With the normalization of the annihilation and creation operators

$$[a_i(p), a_j^\dagger(p')] = (2\pi)^3 2p^0\delta_{ij}\delta^3(p-p'), \quad \text{(A3)}$$

where i and j are the species of a particle, the denominator is

$$\langle a(p)|a(p)\rangle\langle\gamma(k)|\gamma(k)\rangle = 2p^0 2k^0 V^2, \quad \text{(A4)}$$

where $V = (2\pi)^3\delta^3(0)$ is the volume of the system.

Let us assume the axion and photon are moving in z direction and the magnetic field $\vec{B} = \vec{B}(z)$ depends only on z. In the lowest order approximation, the numerator is

$$\langle a(p)|T\exp\left(-i\int H_I dt\right)|\gamma(k)\rangle \simeq -ig_{a\gamma\gamma}\int d^4x B_i(z)\langle a(p)|aF_{0i}|\gamma(k)\rangle. \quad \text{(A5)}$$

For $p^0 = k^0 \equiv \omega$, it reduces to

$$g_{a\gamma\gamma}\omega ST\int dz e^{iqz}\vec{B}(z)\cdot\vec{e}(k), \quad \text{(A6)}$$

where S is the area in xy direction, T is the total time for the conversion, $q = \omega - \sqrt{\omega^2 - m_a^2}$ is the momentum transfer, and $\vec{e}$ is the polarization vector of the final state photon. For high-energy axions, $\omega \gg m_a$, T is equivalent to the length of the system in z direction, L.

Combining the numerator and the denominator, the conversion probability is

$$P(a \to \gamma; \omega) \simeq \frac{\omega^2 g_{a\gamma\gamma}^2 S^2 L^2 |\int dz e^{iqz} \vec{B}(z) \cdot \vec{e}(k)|^2}{4\omega^2 V^2} = \frac{g_{a\gamma\gamma}^2}{4} \left| \int dz e^{iqz} \vec{B}(z) \cdot \vec{e}(k) \right|^2. \quad \text{(A7)}$$

Note that a photon has two polarization modes and we need to sum them up to estimate the conversion probability from an axion to a photon. For the opposite process, the conversion process from a photon to an axion, the same formula holds for the conversion probability. However, once we fix the polarization of the initial state photon, we do not need to sum the polarization modes.

[1] T. Behnke, J. E. Brau, B. Foster, J. Fuster, M. Harrison, J. M. Paterson, M. Peskin, M. Stanitzki, N. Walker, and H. Yamamoto, arXiv:1306.6327.
[2] S. Riemann, P. Sievers, G. Moortgat-Pick, and A. Ushakov, in *Proceedings of the International Workshop on Future Linear Colliders* (2020), arXiv:2002.10919.
[3] R. Peccei and H. R. Quinn, Phys. Rev. Lett. **38**, 1440 (1977).
[4] R. Peccei and H. R. Quinn, Phys. Rev. D **16**, 1791 (1977).
[5] S. Weinberg, Phys. Rev. Lett. **40**, 223 (1978).
[6] F. Wilczek, Phys. Rev. Lett. **40**, 279 (1978).
[7] M. Tanabashi *et al.* (Particle Data Group), Phys. Rev. D **98**, 030001 (2018).
[8] J. E. Kim, Phys. Rev. Lett. **43**, 103 (1979).
[9] M. A. Shifman, A. I. Vainshtein, and V. I. Zakharov, Nucl. Phys. **B166**, 493 (1980).
[10] M. Dine, W. Fischler, and M. Srednicki, Phys. Lett. **104B**, 199 (1981).
[11] A. R. Zhitnitsky, Sov. J. Nucl. Phys. **31**, 260 (1980).
[12] P. Sikivie, Phys. Rev. Lett. **51**, 1415 (1983); **52**, 695(E) (1984).
[13] A. A. Anselm, Yad. Fiz. **42**, 1480 (1985).
[14] K. Van Bibber, N. R. Dagdeviren, S. E. Koonin, A. Kerman, and H. N. Nelson, Phys. Rev. Lett. **59**, 759 (1987).
[15] K. Ehret *et al.* (ALPS Collaboration), Nucl. Instrum. Methods Phys. Res., Sect. A **612**, 83 (2009).
[16] R. Bähre *et al.*, J. Instrum. **8**, T09001 (2013).
[17] G. Ruoso *et al.*, Z. Phys. C **56**, 505 (1992).
[18] R. Cameron *et al.*, Phys. Rev. D **47**, 3707 (1993).
[19] C. Robilliard, R. Battesti, M. Fouche, J. Mauchain, A.-M. Sautivet, F. Amiranoff, and C. Rizzo, Phys. Rev. Lett. **99**, 190403 (2007).
[20] A. S. Chou, W. C. Wester, III, A. Baumbaugh, H. R. Gustafson, Y. Irizarry-Valle, P. O. Mazur, J. H. Steffen, R. Tomlin, X. Yang, and J. Yoo (GammeV (T-969) Collaboration), Phys. Rev. Lett. **100**, 080402 (2008).
[21] A. Afanasev, O. K. Baker, K. B. Beard, G. Biallas, J. Boyce, M. Minarni, R. Ramdon, M. Shinn, and P. Slocum, Phys. Rev. Lett. **101**, 120401 (2008).
[22] R. Ballou *et al.* (OSQAR Collaboration), Phys. Rev. D **92**, 092002 (2015).
[23] T. Inada *et al.*, Phys. Rev. Lett. **118**, 071803 (2017).
[24] W. Gai *et al.* (Positron Working Group), Report on the ILC Positron Source (2018).
[25] Y. Inoue, T. Namba, S. Moriyama, M. Minowa, Y. Takasu, T. Horiuchi, and A. Yamamoto, Phys. Lett. B **536**, 18 (2002).
[26] E. Arik *et al.* (CAST Collaboration), J. Cosmol. Astropart. Phys. 02 (2009) 008.
[27] M. Arik *et al.* (CAST Collaboration), Phys. Rev. Lett. **112**, 091302 (2014).
[28] T. Inada, T. Namba, S. Asai, T. Kobayashi, Y. Tanaka, K. Tamasaku, K. Sawada, and T. Ishikawa, Phys. Lett. B **722**, 301 (2013).
[29] E. K. Akhmedov and A. Y. Smirnov, Found. Phys. **41**, 1279 (2011).
[30] C. Adolphsen *et al.*, arXiv:1306.6328.
[31] Tohoku ILC Project Development Center, Tohoku ILC Civil Engineering Plan (2020).
[32] H. Aihara *et al.* (ILC Collaboration), arXiv:1901.09829.
[33] P. Povinec, M. Betti, A. Jull, and P. Vojtyla, Acta Phys. Slovaca **58**, 1 (2008), http://www.physics.sk/aps/pub.php?y=2008&pub=aps-08-01.
[34] F. Crespi, V. Vandone, S. Brambilla, F. Camera, B. Million, S. Riboldi, and O. Wieland, Nucl. Instrum. Methods Phys. Res., Sect. A **620**, 299 (2010).
[35] R. Caputo *et al.* (AMEGO Collaboration), arXiv:1907.07558.
[36] A. De Angelis *et al.* (e-ASTROGAM Collaboration), Exp. Astron. **44**, 25 (2017).
[37] M. Tavani *et al.* (e-ASTROGAM Collaboration), J. High Energy Astrophys. **19**, 1 (2018).
[38] K. Alharbi, S. Riemann, A. Alrashdi, G. Moortgat-Pick, A. Ushakov, and P. Sievers, in *Proceedings of the International Workshop on Future Linear Colliders* (2021), arXiv:2106.00074.
[39] K. Alharbi, A. Alrashdi, G. Moortgat-Pick, S. Riemann, P. Sievers, and A. Ushakov, JACoW **IPAC2021**, THPAB041 (2021).
[40] L. Di Luzio, F. Mescia, and E. Nardi, Phys. Rev. Lett. **118**, 031801 (2017); Phys. Rev. D **96**, 075003 (2017).
[41] L. Zang, A. Wolski, and I. Bailey, in *Particle Accelerator Conference (PAC 09)* (2010), p. MO6RFP092.